

DOI: 10.24850/j-tyca-2022-03-06

Articles

## **Forecast of meteorological droughts with neural networks in Sonora watershed, Mexico**

## **Pronóstico de sequías meteorológicas usando redes neuronales artificiales en la cuenca del río Sonora, México**

Claudio César Hernández-Vásquez<sup>1</sup>, ORCID: <https://orcid.org/0000-0003-3931-8780>

Laura Alicia Ibáñez-Castillo<sup>2</sup>, ORCID: <https://orcid.org/0000-0001-9287-655X>

Ramón Arteaga-Ramírez<sup>3</sup>, ORCID: <https://orcid.org/0000-0001-9459-3588>

Alejandro Ismael Monterroso-Rivas<sup>4</sup>, ORCID: <https://orcid.org/0000-0003-4348-8918>

Rocío Cervantes-Osornio<sup>5</sup>, ORCID: <https://orcid.org/0000-0003-2597-4517>

<sup>1</sup>Universidad Autónoma Chapingo, Texcoco, México,  
[claudiohdezvqz@gmail.com](mailto:claudiohdezvqz@gmail.com)

<sup>2</sup>Universidad Autónoma Chapingo, Texcoco, México, libacas@gmail.com

<sup>3</sup>Universidad Autónoma Chapingo, Texcoco, México,  
arteagarr@gmail.com

<sup>4</sup>Universidad Autónoma Chapingo, Texcoco, México, aimrivas@gmail.com

<sup>5</sup>Campo Experimental Valle de México-INIFAP, Coatlinchán, México,  
rcervanteso@hotmail.com

Corresponding author: Claudio César Hernández-Vásquez,  
claudiohdezvqz@gmail.com

## Abstract

Droughts are hydrometeorological hazards that are characterized by an abnormal and persistent humidity deficit. In the last years, this hazard has been present more frequently and with more severity levels, producing negative impacts on the ecosystem, agriculture, livestock, and society. Therefore, its monitoring and forecast must be part of integral planning, preparation, and mitigation of its adverse effects at local, regional, and national levels. In Mexico, most of the drought studies are focused on characterization and analysis. Thus, in this research, we evaluated the application of artificial neural networks (ANN) to forecast the meteorological droughts in the medium and high parts of the Sonora River watershed. SPI and SPEI indexes were used, on scales of 3, 6, 12, and, 24 months, for the 1974 to 2013 period of years. Forecast results

showed that ANN has a satisfactory level of prediction, with an average determination coefficient ( $R^2$ ) in the validation phase, of 0.76. It was observed that the statistical efficiency of SPEI was better than that of SPI and that this efficiency increased with the longer temporal scale; maybe because in a short term, climate variability is greater.

**Keywords:** SPI, SPEI, multilayer perceptron (MLP), cross-validation, resilient propagation (RPROP).

## Resumen

Las sequías son un fenómeno hidrometeorológico extremo que se caracteriza por la deficiencia de humedad de manera anormal y persistente. En los últimos años, este fenómeno se ha presentado con mayor frecuencia y con niveles de gravedad cada vez más intensos, lo que ha provocado numerosos impactos negativos en los sistemas ecológicos, agrícolas, ganaderos y sociales. Por lo tanto, su monitoreo y pronóstico deben ser parte integral de la planeación, preparación y mitigación de sus efectos adversos a nivel local, regional e incluso nacional. En México, los estudios se han enfocado mayoritariamente en la caracterización y el análisis de los eventos de sequía, por lo que el objetivo de este estudio fue evaluar la aplicabilidad de las redes neuronales artificiales (RNA) para pronosticar las sequías meteorológicas en la parte media y alta de la cuenca del río Sonora, México. Para ello se utilizaron los índices SPI y SPEI a escalas temporales de 3, 6, 12 y 24 meses, para el periodo de 1974 a 2013. De manera general, los resultados mostraron

que las habilidades predictivas de los modelos de RNA fueron satisfactorias, con un coeficiente de determinación ( $R^2$ ) promedio de 0.76 en la etapa final de validación de los modelos. Se observó que el rendimiento estadístico de los modelos para el pronóstico del SPEI fue superior al SPI y que éste aumentaba conforme la escala temporal era mayor, probablemente debido a que a corto plazo existe mayor variabilidad de las condiciones climáticas.

**Palabras clave:** SPI, SPEI, perceptrón multicapa (MLP), validación cruzada, propagación resiliente (RPROP).

Received: 19/02/2021

Accepted: 11/05/2021

## Introduction

Droughts are classified as meteorological, agricultural, hydrological, and socioeconomic (Wilhite & Glantz, 1985). Meteorological droughts are distinguished by a decrease in precipitation relative to the historical mean of a given period; its intensification and prolongation lead to the

appearance of the other types of drought (Ravelo, Sanz-Ramos, & Douriet-Cárdenas, 2014). For its study and monitoring, indexes have been used as tools to evaluate their main characteristics, such as intensity and duration. Among the most used indexes are SPI (Standard Precipitation Index) and SPEI (*Standard Precipitation Evapotranspiration Index*). The former, calculated based on monthly precipitation registers, was proposed by McKee, Doesken, and John (1993) and is recommended by the World Meteorological Organization (OMM & GWP, 2016). SPEI was proposed by Vicente-Serrano, Beguería, and López-Moreno (2010) based on SPI; as an entry datum, it uses a monthly water balance that results from subtracting potential evapotranspiration from precipitation. Both indexes give positive and negative values that are correlated directly with events of humidity or drought and being of a probabilistic nature, describe ideal characteristics for forecast and risk assessment (Anshuka, van Ogtrop, & Willem-Vervoort, 2019), which is important in decision-making for timely action to prevent, reduce or mitigate the adverse effects of this extreme phenomenon by providing anticipated information of its intensity, duration and spatial dispersion (Castillo-Castillo, Ibáñez-Castillo, Valdés, Arteaga-Ramírez, & Vázquez-Peña, 2018).

Mishra and Singh (2011) discuss the advantages, limitations, and applications of diverse methodologies for drought forecasting. Among the methodologies they describe are artificial neural networks (ANN), an idea proposed by McCulloch and Pitts (1943) more than seventy years ago and has had a great resurgence since the early 1990s due to the development

of more sophisticated algorithms and more powerful computational tools. In hydrology, for example, ANN has been used successfully to forecast precipitation, model the rain-runoff process, forecast flows, and model groundwater (ASCE, 2000). Regarding drought forecasting, Achour *et al.* (2020) mention that artificial intelligence models, such as neural networks, can produce better results than conventional techniques like the Markov chains, regression methods, or integrated moving average autoregressive linear stochastic (ARIMA) or seasonal autoregressive integrated moving average (SARIMA) models.

ANN are information processing systems whose structure and functioning are inspired by biological neural networks. They can learn, remember and generalize from examples or training patterns like a human brain (ASCE, 2000). ANN are effective tools for modeling non-linear processes. They use non-parametric regression techniques to relate the input and output of the system without the need to understand the physical process involved (Djerbouai & Souag-Gamane, 2016). Generally, information processing in ANN occurs in individual elements called nodes or neurons ( $k$ ). These neurons receive a given number ( $n$ ) of inputs ( $x_1, x_2, x_3, \dots, x_n$ ), which are weighted by a determined number of adaptable constants called synaptic weights ( $w_1, w_2, w_3, \dots, w_n$ ). Once the inputs have been weighted, they are summed in the nucleus of the neuron ( $\Sigma$ ) to produce what is known as net input ( $u_k$ ), which is evaluated by an activation function ( $\varphi$ ) and, in this way, the output signal of the neuron ( $y_k$ ) is generated. During information processing, an external parameter

known as bias ( $b_k$ ) is included, whose value increases or decreases the net input depending on whether it is positive or negative, respectively (Haykin, 1998). In mathematical terms, a neuron  $k$  can be described with equations (1) and (2):

$$u_k = \sum_{i=1}^n x_i w_{ki} = x_1 w_{k1} + x_2 w_{k2} + x_3 w_{k3} + \cdots + x_n w_{kn} \quad (1)$$

$$y_k = \varphi(u_k + b_k) \quad (2)$$

Recent studies in different regions of the world have demonstrated that ANN models are effective in estimating and forecasting droughts using analysis of indexes such as SPI (Azizi, Tavakoli, Karimi, & Faramarzi, 2019; Choubin, Malekian, & Golshan, 2016; El-Ibrahimi & Baali, 2018) and SPEI (Mouatadid, Raj, Deo, & Adamowski, 2018; Soh, Koo, Huang, & Fung, 2018; Zhang, Chen, Xu, & Ou, 2019). In Mexico, studies have focused mainly on the characterization and analysis of drought events, and few are developed in the area of forecasting using ANN as does the work of Ravelo *et al.* (2014), who forecasted drought intensity in the North Pacific Basin Organization using SPI and the Palmer Drought Severity Index (PDSI). They obtained Pearson coefficients equal to or higher than 0.64 for one-month forecasts and 0.60 for three-month forecasts, a good correlation between the calculated drought index and the value predicted using neural networks. Also, Villazón-Bustillos *et al.*

(2016) used NARX (*Nonlinear Autoregressive Exogenous*) neural networks to analyze rainfall patterns and predict the following drought events in the northwestern region of the state of Chihuahua. With NARX they obtained rainfall prediction errors between 2.35 and 12.16 mm, while with ARIMA models, the prediction errors were larger, oscillating between 4.85 and 56.45 mm. In the Sonora River Basin, there are no previous studies similar to the study we propose, and predicting drought is important for the basin, first, because it is within the boundaries of Hermosillo, the state capital and one of the most populated cities of the state, and second because, according to Oertel *et al.* (2018), the population has undergone major growth in recent years and has resulted in higher water demand for agricultural, urban and industrial use. On the other hand, one of the most important irrigation districts, Costa de Hermosillo, is found here, where the largest user of available water in the basin is the agricultural sector (Palma, González, & Cruickshank, 2015). Moreover, the analysis carried out by Hernández-Vásquez, Ibáñez-Castillo, Gómez-Díaz, and Arteaga-Ramírez (2021) of meteorological droughts in the study area indicates that drought intensity and frequency have increased, identifying important events in 1997, 1999, 2000 and 2011 to 2013. In this context, knowledge of future conditions of droughts in the study basin would contribute to creating contingency plans to deal with the negative impact of this phenomenon and prevent serious economic, social and environmental consequences. For this reason, the objective of this study was to evaluate the applicability of ANN to meteorological drought forecasting in the middle and high parts of the

Sonora River Basin, Mexico. To this end, the SPI and SPEI indexes were used at temporal scales of 3, 6, 12, and 24 months for the period 1974 to 2013.

## **Materials and methods**

### **Study area**

The study area has an area of 21,220 km<sup>2</sup> covering the middle and upper parts of the Sonora River Basin, which is located in the central-northeastern region of the state of the same name (28°5'19.23" and 30° 59' 18.56" N; 109° 52' 8.92" and 111° 37' 52.81" W) (Figure 1).

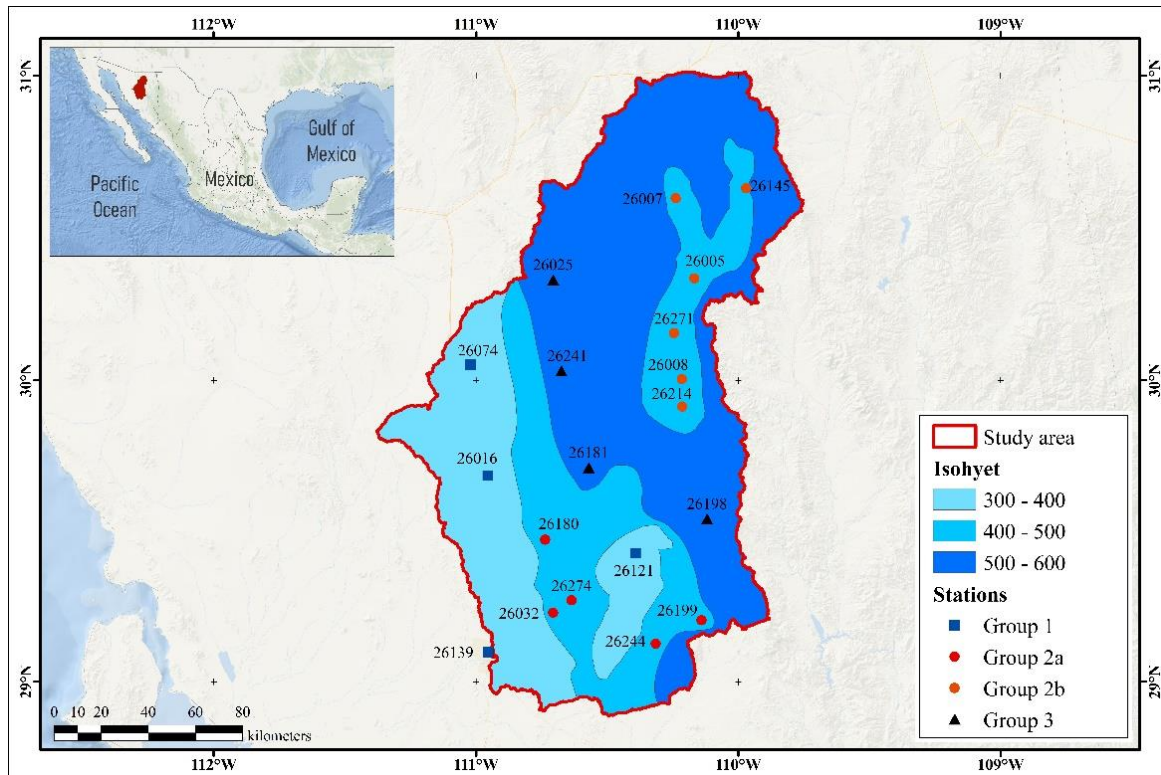


**Figure 1.** Location of the study area and weather stations grouped by homogeneous precipitation regions.

Based on climatological data from 19 stations located within the study area, mean annual precipitation fluctuates between 300 and 600 mm with two periods of rain. The first and most important in summer is associated with the North American monsoon and the second in the winter is produced by the impact of the vortexes. The mean annual temperature varies from 12 °C in the mountainous zones to 24 °C in the area surrounding the city of Hermosillo.

## Climatological information

We used the series of monthly data on precipitation, maximum temperature, and minimum temperature from 19 weather stations (Figure 1, Table 1) of the National Meteorological Service (SMN, 2019). The data cover a period of 40 years, from January 1974 to December 2013. Complete series were required, and lacking data were estimated by the Inverse Distance Weighting method, suggested by the World Meteorological Organization (OMM, 2011), in which absent data are estimated with observed values in four or, failing that, three or two nearby stations (Campos-Aranda, 1998).

**Table 1.** Weather stations are located in the study area.

<b>Station</b>	<b>Altitude</b>	<b>Latitude</b>	<b>Longitude</b>	<b>P</b>	<b>Tmax</b>	<b>Tmin</b>	<b>Dat. Est.</b>	<b>Group/ Isohyet</b>	
		<b>(N)</b>	<b>(W)</b>	<b>(mm)</b>	<b>(°C)</b>	<b>(°C)</b>	<b>(%)</b>		
26139	Hermosillo II	221	29°05'56"	110°57'14"	363.5	32.2	17.7	0.3	1

26121	Ures	385	29°25'37"	110°23'31"	375.6	31.8	9.1	12.1	(300 -400 mm)
26016	Carbo	464	29°41'03"	110°57'18"	374.6	31.2	13.0	4.9	
26074	Querobabi	661	30°03'02"	111°01'17"	394.0	31.2	11.3	12.1	
26032	El Orégano	279	29°13'48"	110°42'21"	410.6	33.8	14.1	6.9	
26274	Topahue	300	29°16'15"	110°38'09"	418.6	33.1	12.9	22.4	
26180	El Cajón	390	29°28'19"	110°44'09"	414.2	32.1	11.7	2.3	2a (400 - 500 mm)
26244	Rancho Viejo	450	29°07'37"	110°18'54"	458.6	31.1	12.4	28.1	
26199	Pueblo de Álamos	589	29°12'15"	110°08'25"	498.8	30.8	11.7	15.8	
26214	Huepac	644	29°54'46"	110°12'47"	496.5	30.1	9.7	19.7	
26008	Banamichi	675	30°00'12"	110°12'54"	459.7	30.7	13.3	1.7	
26271	Sinoquipe	740	30°09'20"	110°14'42"	504.5	30.5	11.6	39.8	2b (400 - 500 mm)
26005	Arizpe	836	30°20'08"	110°10'03"	474.5	29.4	10.0	31.9	
26007	Bacanuchi	1049	30°35'56"	110°14'18"	489.1	28.0	7.4	6.2	
26145	Bacoachi	1049	30°37'54"	109°58'12"	465.5	28.0	8.2	35.3	
26198	Mazocahui	449	29°32'26"	110°07'09"	517.6	31.4	11.2	22.1	
26181	Rayón	560	29°42'38"	110°34'14"	500.5	30.6	11.8	7.7	
26241	Meresichic	712	30°01'50"	110°40'30"	521.8	28.5	11.0	38.9	3 (500 - 600 mm)
26025	Cucurpe	853	30°19'50"	110°42'21"	524.7	29.6	10.3	10.4	

P= Mean annual precipitation, Tmax= Average maximum temperature,

Tmin= Average minimum temperature, Dat. Est. = Estimated data

In the study area, isohyets, or precipitation homogeneous regions, were generated (Figure 1, Table 1), and thus the stations were grouped in such a way that they shared similar patterns in the annual rainfall registers. For each station of each of the regions, SPI and SPEI were calculated at temporal scales of 3, 6, 12, and 24 months, following the methodologies developed by McKee *et al.* (1993) and Vicente-Serrano *et al.* (2010), respectively. Finally, for each region temporal series were obtained with the mean values of each of the indexes and temporal scales used. The calculations were conducted in RStudio (2018) using the software SPEI.R of Beguería and Vicente-Serrano (2017). For more information on the calculations and analyses of droughts in the study area, see Hernández-Vásquez *et al.* (2021).

## Artificial Neural Networks (ANN)

For the prediction of the SPI and SPEI indexes at different temporal scales, different multi-layer neural network architectures were evaluated. The

number of neurons in the input layer ( $n=3$  to 12) was increased unitarily, and in the hidden layer (from  $n$  to  $2n + 1$ ) the parameters of each model were estimated using the training algorithm *RPROP+* or *RPROP-*. Cross-validation of  $k=10$  iterations was used to avoid overfitting and to increase the generalization capacity of each model, as we describe in detail below.

Although different ANN models exist, in this study we adopted the multi-layer perceptron (MLP) model with feed-forward connections for two reasons. First, it is the most popular architecture and, second, it is recognized as one of the most powerful for estimation of hydrological time series (Achour *et al.*, 2020). MLP models were developed based on a three-layer architecture with different levels and variable quantities of neurons in each layer. In the input layer, the number of neurons was equal to the observations delayed in time  $t-n$ , where  $n$  is the delays that varied 3 to 12 months of the series with SPI or SPEI values in each of the time scales of 3, 6, 12 or 24 months. In the output layer, a single neuron was assumed since a single variable was predicted ( $SPI_{t+1}$  or  $SPEI_{t+1}$ ). The optimal density of the neurons in the hidden layer was determined by testing different quantities, from  $n$  to  $2n + 1$  in unitary increments (Mishra & Desai, 2006).

To obtain the output value of the neuron, it was necessary to determine its activation value. For this reason, the sigmoidal function was used; this possesses a continuous range of values within the intervals [0, 1] and is reported in the literature as one of the non-linear functions most used in the construction of neural networks (Khan, Muhammad, & El-

Shafie, 2018). It is expressed by Equation (3), where  $u$  represents the weighted sum of the inputs for the neuron and  $e$  denotes the exponential function:

$$\varphi(u) = \frac{1}{1+e^{-u}} \quad (3)$$

The ANN input values were normalized so that they were found within the activation function range, using the following equation (Bari-Abarghouei, Reza-Kousari, & Asadi-Zarch, 2013):

$$X_{nor} = \frac{X_0 - X_{min}}{X_{max} - X_{min}} \quad (4)$$

Where  $X_0$  corresponds to the original value of the drought index,  $X_{min}$  and  $X_{max}$  represent the minimum and maximum values in the series of original data, and  $X_{nor}$  is the normalized value.

During the learning stage, the synaptic weights of the neural network were adjusted using the algorithms RPROP+ (Riedmiller, 1994) and RPROP- (Riedmiller & Braun, 1993), which refers to the resilient propagation (RPROP) learning method which considers backpropagation of error with and without regression in weight, respectively. This method is considered a superior version of backpropagation because it solves slow converging problems and weights of the network stagnated around local

optimal (Prasad, Singh, & Lal, 2013) and is recognized by Ortíz, Villa, and Velásquez (2007) as one of the most appropriate algorithms for training artificial neural networks.

Velásquez, Villa, and Souza (2010) mention that MLP has some inconveniences, such as overfitting, in which the network memorizes the training data and even the noise they contain, decreasing its ability to provide a correct response because of data that were not used during training, that is, in the validation or testing stage (Günther & Fritsch, 2010). To control overfitting, in our study, we used the cross-validation technique, for which the entire set of data was divided into  $k = 10$  subsets, one of which served as validation data and the rest as training data. This process was repeated iteratively with each of the possible validation subsets (Martín-del-Brio & Sanz-Molina, 2001; Velásquez, Fonnegra, & Villa, 2013).

The ANN that led to the least mean square error (*MSE*) (Gómez-Guerrero & Aguayo-Arias, 2019; Vargas-Castañeda, Ibáñez-Castillo, & Arteaga-Ramírez, 2015) during validation was conserved as the optimal architecture and its performance in the prediction of drought indexes was evaluated by diverse measures of goodness of fit as the coefficient of determination ( $R^2$ ) (Cervantes-Osornio, Arteaga-Ramírez, Vázquez-Peña, Ojeda-Bustamante, & Quevedo-Nolasco, 2013; Gallegos-Cedillo, Arteaga-Ramírez, Vázquez-Peña, & Juárez-Méndez, 2016) and Nash-Sutcliffe efficiency (E) (Djerbouai & Souag-Gamane, 2016; Laqui *et al.*, 2019; Soh

*et al.*, 2018). The calculation of *MSE*,  $R^2$  and *E* is shown in equations (5), (6), and (7), respectively:

$$MSE = \frac{1}{N} \sum_{i=1}^N (Obs_i - Est_i)^2 \quad (5)$$

$$R^2 = \frac{[\sum_{i=1}^N (Est_i - \bar{Est})(Obs_i - \bar{Obs})]^2}{[\sum_{i=1}^N (Est_i - \bar{Est})^2][\sum_{i=1}^N (Obs_i - \bar{Obs})^2]} \quad (6)$$

$$E = 1 - \frac{\sum_{i=1}^N (Obs_i - Est_i)^2}{\sum_{i=1}^N (Obs_i - \bar{Obs})^2} \quad (7)$$

Where *Obs* are observed data and  $\bar{Obs}$  is the observed mean, *Est* is estimated data, and  $\bar{Est}$  is the estimated mean; *N* is the number of observations in the period considered. For the *MSE*, a value equal to zero and  $R^2$  and *E* equal to 1.0 indicates a perfect model fit with an excellent capacity for predicting droughts.

To develop different ANN models, select the optimal architecture, and forecast drought, we used the software package Neuralnet developed by Günther and Fritsch (2010) for RStudio (2018).

## Results and discussion

The results are presented by groups of weather stations that make up each rainfall homogeneous region, as indicated in Table 1. For each index (SPI or SPEI) and temporal scale (3, 6, 12, or 24 months) of each group, we tested and evaluated a total of 1,900 ANN models, as specified in Table 2 and we selected that which had the least *MSE* during model validation.

**Table 2.** Artificial neural networks for drought forecasting.

Neurons in the layer of				Training algorithms	<b>Cross-Validation</b>	<b>Different ANN models</b>
Input	Hidden		Output			
(n)	(n	a	2n + 1)	(SPI o SPEI)	(RPROP+ y RPROP-)	k=10
3	3	-	7	1	2	100
4	4	-	9	1	2	120
5	5	-	11	1	2	140
6	6	-	13	1	2	160
7	7	-	15	1	2	180
8	8	-	17	1	2	200
9	9	-	19	1	2	220
10	10	-	21	1	2	240

11	11	-	23	1	2	10	260
12	12	-	25	1	2	10	280

Table 3 presents the neural network models for group 1, which has a better statistical yield. The results, in general, show good model performance. In the training stage, the average efficiency for a temporal scale of three months was 0.80, while for 24 months, it was 0.96. Regardless of the drought index evaluated, during the validation stage, efficiency decreased in all cases, but when trained neural networks were tested and validated in the entire data set, efficiencies increased; the lowest was obtained for 3-month scales ( $SPI = 0.78$  and  $SPEI = 0.79$ ) and the highest in 24-month scales with values of 0.96 and 0.97 for SPI and SPEI, respectively.

**Table 3.** Optimal neural network models for group 1.

Index	Optimal architecture	Training algorithm	Training			Validation			Complete series		
			MSE	E	R <sup>2</sup>	MSE	E	R <sup>2</sup>	MSE	E	R <sup>2</sup>
SPI 3	10-14-1	RPROP+	0.009	0.79	0.79	0.012	0.48	0.54	0.143	0.78	0.78
SPI 6	7-10-1	RPROP+	0.007	0.82	0.82	0.004	0.74	0.75	0.125	0.82	0.82
SPI 12	10-14-1	RPROP+	0.004	0.91	0.91	0.002	0.84	0.86	0.062	0.91	0.91
SPI 24	8-17-1	RPROP-	0.002	0.96	0.96	0.001	0.74	0.80	0.031	0.96	0.96

SPEI 3	10-13-1	<i>RPROP-</i>	0.009	0.80	0.80	0.009	-0.07	0.51	0.145	0.79	0.79
SPEI 6	7-12-1	<i>RPROP-</i>	0.007	0.85	0.85	0.004	0.53	0.63	0.096	0.86	0.86
SPEI 12	12-15-1	<i>RPROP-</i>	0.003	0.94	0.94	0.004	0.37	0.62	0.045	0.94	0.94
SPEI 24	10-15-1	<i>RPROP-</i>	0.002	0.97	0.97	0.001	0.95	0.96	0.021	0.97	0.97

El-Ibrahimi and Baali (2018) explored short-term (SPI 3) and long-term (SPI 12) prediction of drought conditions at the weather stations Fez-DRH and Ain Bittit located in the Saïss plains of northern Morocco, using six models: adaptive neuro-fuzzy inference system (ANFIS), multi-layer perceptron artificial neural networks (ANN), regression vector systems (RVS), and each of these combined with the Wavelet transform method. In general, the results obtained showed that the ANFIS-Wavelet models had better predictions, in terms of  $R^2$ , for both stations. Moreover, the results for SPI 12 are better than those expected for SPI 3 in all cases. Yields of  $R^2$  obtained in the Fez-DRH station with ANN and ANN-Wavelet for SPI 12 were 0.74 and 0.87 in training and 0.80 and 0.83 in validation, respectively. These results are lower than those obtained in our study. Castillo-Castillo *et al.* (2018) conducted SPI and SPEI forecasting for 14 weather stations in the Fuerte River Basin located in Northwestern Mexico using the algorithm of the discrete Kalman filter (DKF). Their results coincide with those of our study, obtaining better forecasts for 12- and 24-month scales when predicting SPEI. The efficiency of their forecasts

for 12 and 24 months was 0.92 and 0.96, slightly lower than those achieved in our study.

Figure 2 presents the architecture of the ANN model that had the statistically highest performance ( $MSE$ ,  $E$ , and  $R^2$ ) in group 1, with a delay time of 10 months in the input layer, a hidden layer of 15 neurons, and one neuron in the output layer, representing the predicted value of the SPEI index at a temporal scale of 24 months. Figure 3 shows its yield, according to the  $R^2$ , during the stage in which the model was constructed and during its validation.

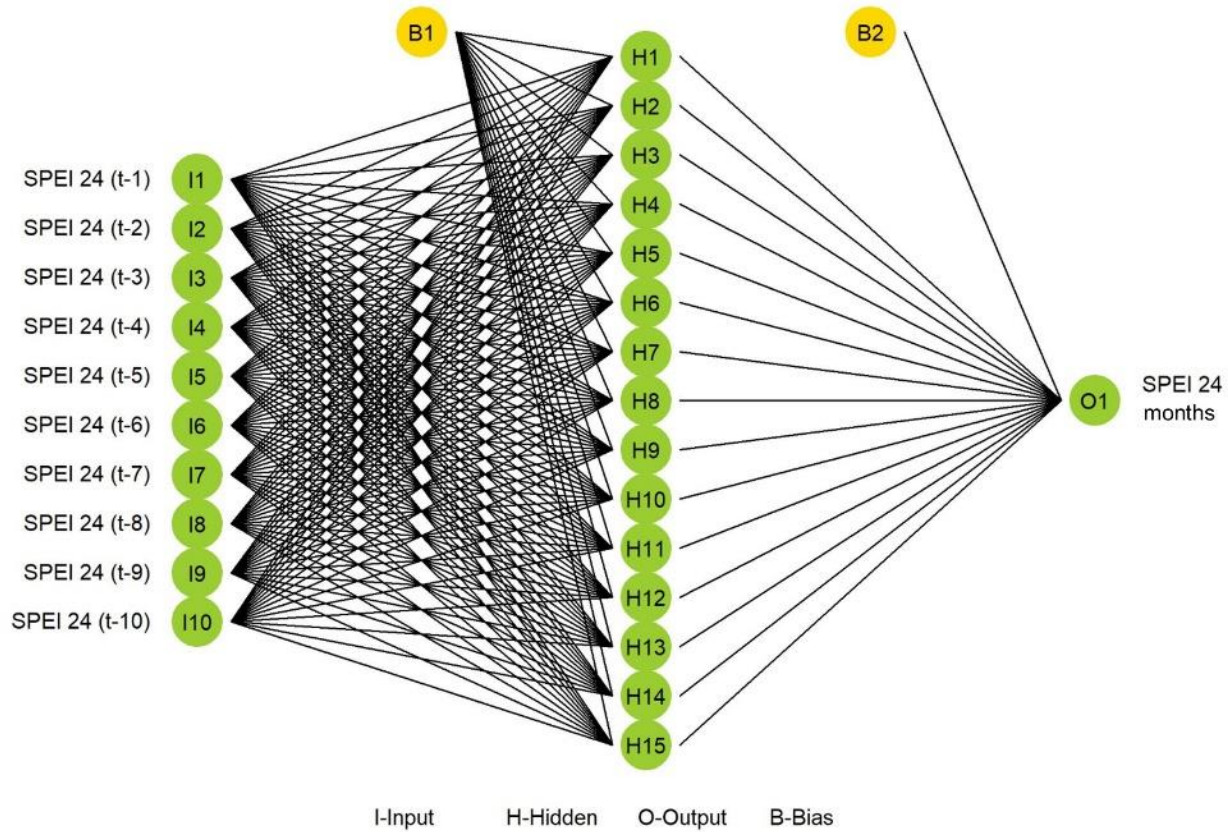


**Figure 2.** The architecture of the neural network for SPEI 24 of group 1.

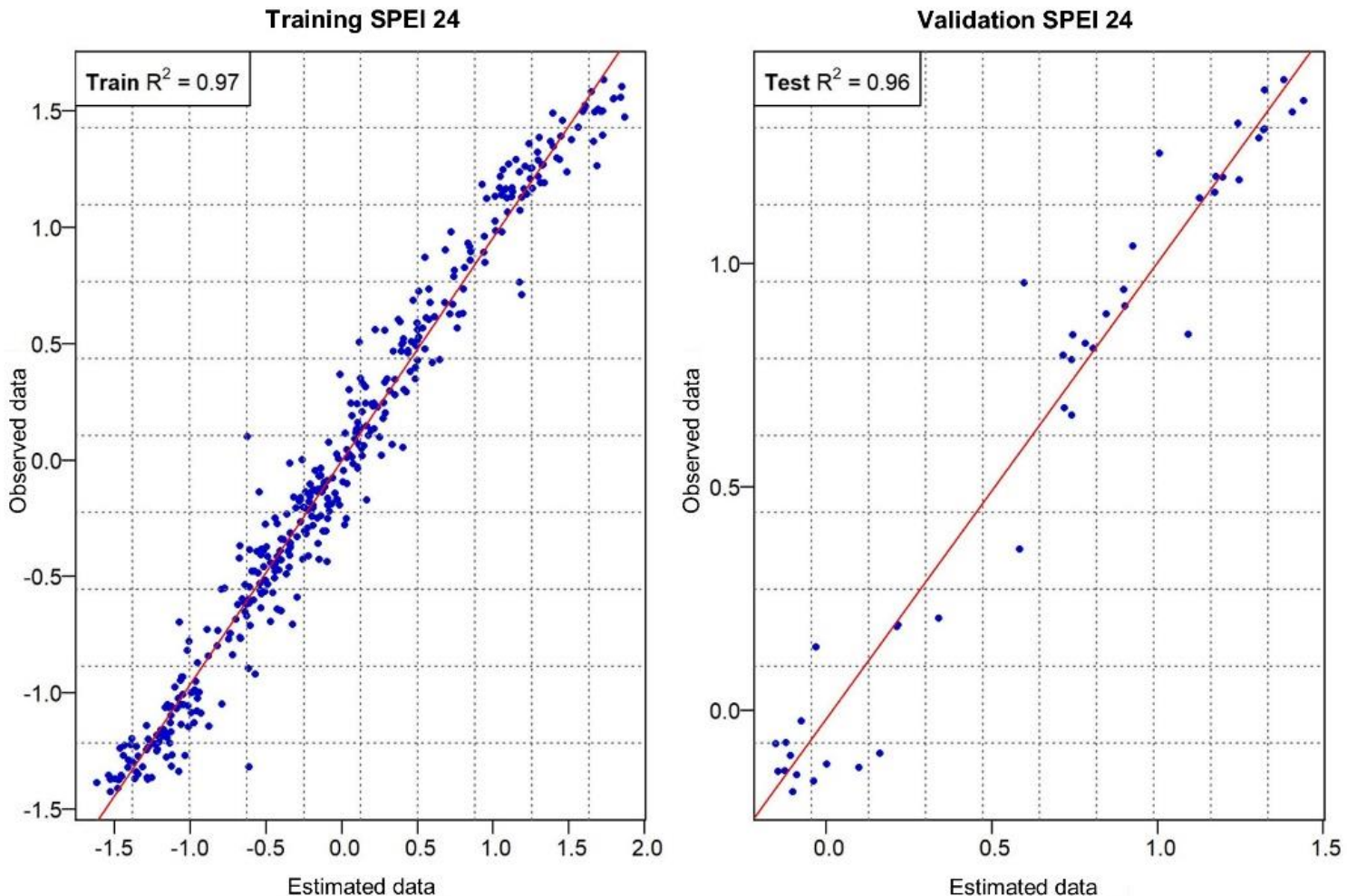


**Figure 3.** Training and validation of the neural network for SPEI 24 of group 1.

In the group of stations denominated 2a, the optimal models had efficiencies of 0.59 to 0.96 during training; the lowest was achieved with SPI 3 data and the highest with SPEI 24 data. During validation, efficiency did not vary significantly, reaching values of 0.60 and 0.96, respectively

(Table 4). A study conducted by Mouatadid *et al.* (2018) applied a machine extreme learning model (ELM), a multiple linear regression model (MLR), an artificial neural network (ANN), and the least squares support vector regression model (LSSVR) to predict SPEI at six weather stations of a region susceptible to droughts in eastern Austria. The results revealed a higher predictive precision of the ANN compared with the other three techniques, and the forecasts were better evaluated in SPEI 12 than in SPEI 3 with an  $R^2$  of 0.89 during the validation stage, very similar to that obtained in our study ( $R^2 = 0.88$ ). Likewise, in the work of Villazón-Bustillos *et al.* (2016), NARX type neural networks were superior to ARIMA models, obtaining better precision in forecasting precipitation in the northwestern region of the state of Chihuahua. Predictive errors with NARX models oscillated between 2.35 and 12.16 mm, while with ARIMA models they fluctuated between 4.85 and 56.45 mm.

**Table 4.** Optimal neural network models for group 2a.

Index	Optimal architecture	Training algorithm	Training			Validation			Complete series		
			MSE	E	R <sup>2</sup>	MSE	E	R <sup>2</sup>	MSE	E	R <sup>2</sup>
SPI 3	3-5-1	RPROP-	0.015	0.59	0.59	0.008	0.60	0.60	0.288	0.59	0.59
SPI 6	11-18-1	RPROP+	0.005	0.85	0.85	0.003	0.52	0.58	0.115	0.85	0.85
SPI 12	10-18-1	RPROP-	0.004	0.90	0.90	0.003	0.89	0.89	0.075	0.90	0.90
SPI 24	4-4-1	RPROP-	0.003	0.94	0.94	0.001	0.92	0.92	0.038	0.95	0.95

SPEI 3	12-12-1	<i>RPROP-</i>	0.007	0.85	0.85	0.009	0.67	0.69	0.125	0.84	0.84
SPEI 6	12-22-1	<i>RPROP-</i>	0.003	0.93	0.93	0.007	0.58	0.75	0.059	0.93	0.93
SPEI 12	10-19-1	<i>RPROP-</i>	0.004	0.93	0.93	0.003	0.88	0.88	0.054	0.93	0.93
SPEI 24	11-11-1	<i>RPROP+</i>	0.002	0.96	0.96	0.001	0.96	0.97	0.029	0.96	0.96

Evaluation of ANN model performance with the complete series of data obtained  $R^2$  values of 0.59 to 0.95 for SPI and 0.84 to 0.94 for SPEI, increasing with longer temporal scales. The architecture 11-11-1 with the training algorithm *RPROP+* achieved the highest average yield (average  $R^2 = 0.97$ ) to predict the behavior of the drought using SPEI at 24 months, while the lowest yield was for SPI 3 with the 3-5-1 network architecture (Figure 4) and the algorithm *RPROP-*, with which an  $R^2$  of 0.59 was obtained during training and 0.60 in model validation (Figure 5).

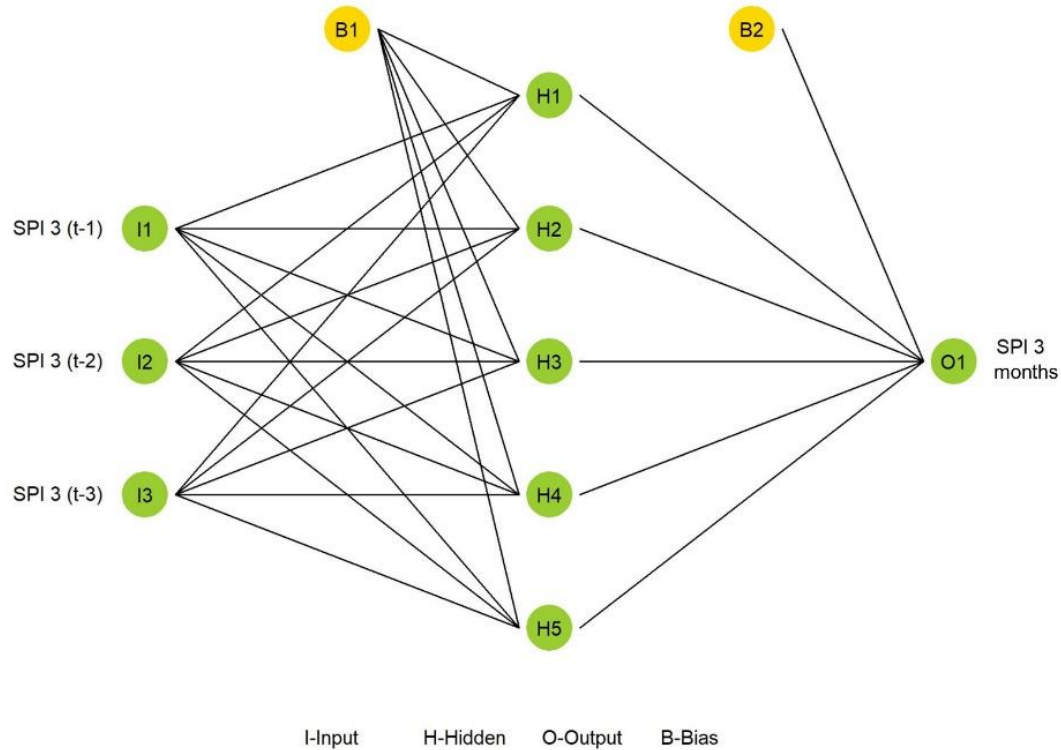


**Figure 4.** The architecture of the neural network for SPI 3 of group 2a.

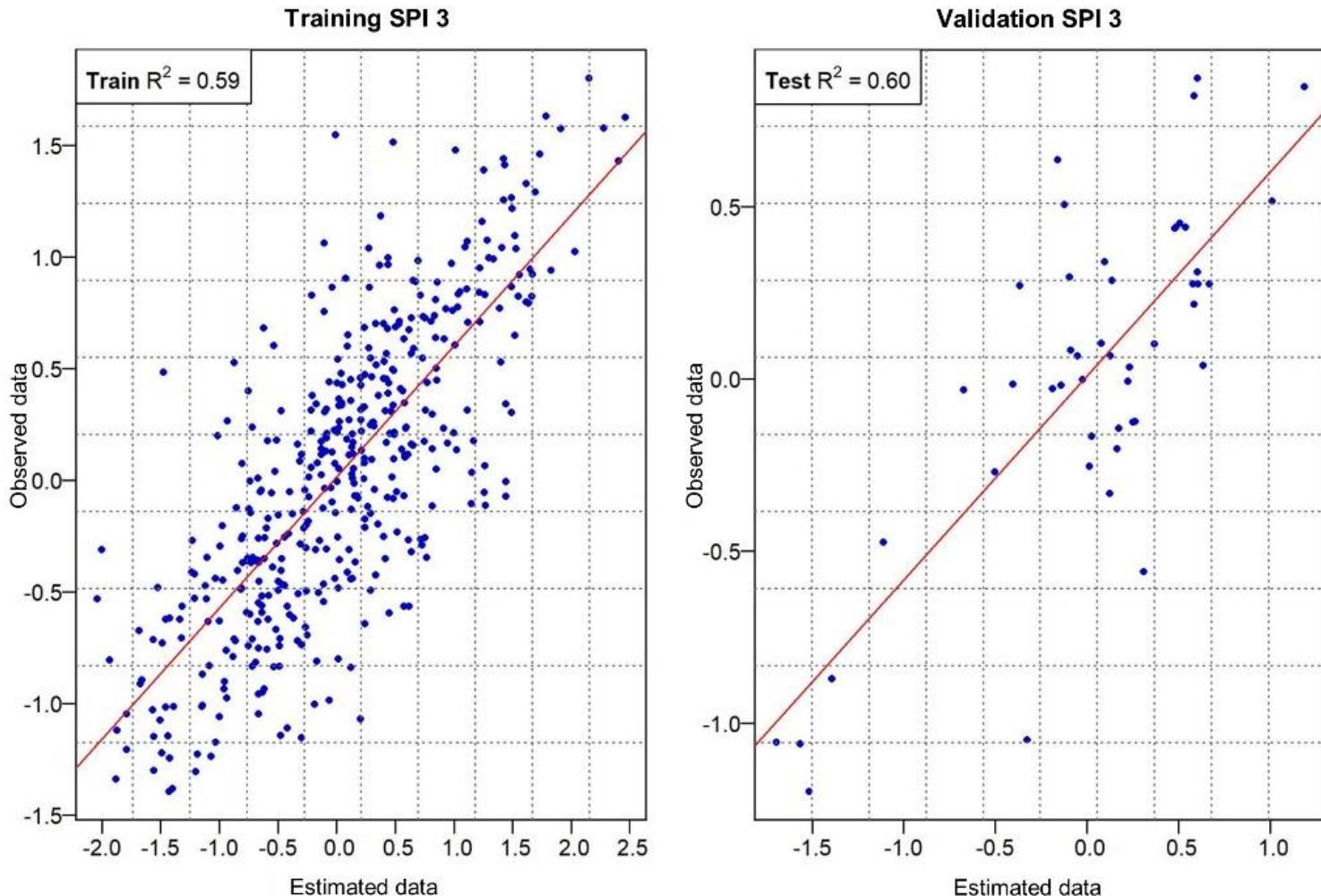


**Figure 5.** Training and validation of the neural network for SPI 3 of group 2a.

Results of the experimentation in group 2b are presented in Table 5. With longer temporal scales of SPI or SPEI, model yield increased, as indicated by *MSE*,  $R^2$  and *E*. These results agree with Rezaeian-Zadeh and

Tabari (2012), who predicted SPI at 3, 6, 9, 12, and 24 months at five weather stations in Iran; their results indicate that the MLP predicted SPI 24 and SPI 12 more precisely than SPI at smaller time scales.

**Table 5.** Optimal neural network models for group 2b.

Index	Optimal architecture	Training algorithm	Training			Validation			Complete series		
			MSE	E	R <sup>2</sup>	MSE	E	R <sup>2</sup>	MSE	E	R <sup>2</sup>
SPI 3	7-8-1	RPROP-	0.013	0.64	0.64	0.007	0.74	0.74	0.271	0.65	0.65
SPI 6	11-21-1	RPROP-	0.005	0.84	0.85	0.009	0.11	0.59	0.126	0.84	0.84
SPI 12	8-13-1	RPROP-	0.006	0.86	0.86	0.003	0.62	0.68	0.100	0.86	0.86
SPI 24	9-17-1	RPROP+	0.004	0.93	0.93	0.002	0.73	0.79	0.050	0.93	0.93
SPEI 3	7-15-1	RPROP-	0.011	0.78	0.78	0.013	0.45	0.56	0.181	0.77	0.77
SPEI 6	7-9-1	RPROP+	0.008	0.86	0.86	0.005	0.72	0.74	0.112	0.86	0.86
SPEI 12	9-10-1	RPROP-	0.005	0.91	0.91	0.003	0.81	0.84	0.065	0.92	0.92
SPEI 24	11-20-1	RPROP-	0.002	0.97	0.97	0.001	0.89	0.91	0.023	0.97	0.97

In our study, the highest efficiencies in training were 0.93 for SPI and 0.97 for SPEI, both at scales of 24 months. *MSE* did not surpass 0.013 in any of the forecasts, so we can assert that the results are favorable in the training stage. In model validation, the measures of goodness of fit produced *R<sup>2</sup>* values above 0.56 in all cases, and efficiencies of 0.11 for

SPI 6 to 0.89 for SPEI 24, while in model evaluation with complete data series efficiencies and  $R^2$  prediction of drought indexes were above 0.65, with a maximum of 0.97 for SPEI 24.

Figure 6 shows the architecture obtained with the statistics that had the best performance during training and validation, which were carried out simultaneously by applying the cross-validation technique. Figure 7 shows that  $R^2$  during training was 0.97 and 0.91 in the validation model, achieved by the architecture of 11 neurons in the input layer and 20 neurons in the hidden layer. The output neuron obtained was the prediction of the SPEI index at 24 months.

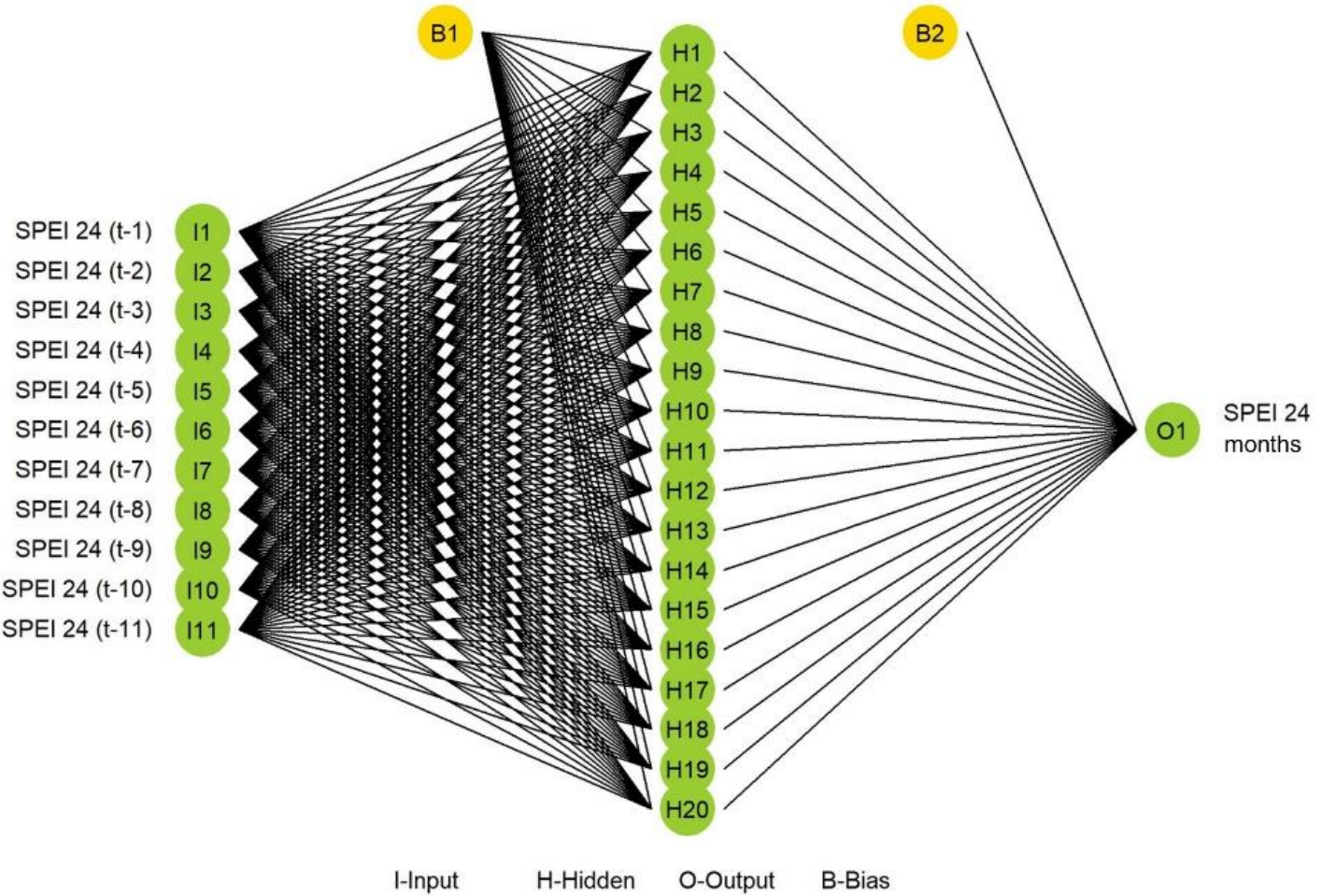


**Figure 6.** The architecture of the neural network for SPEI 24 of group 2b.

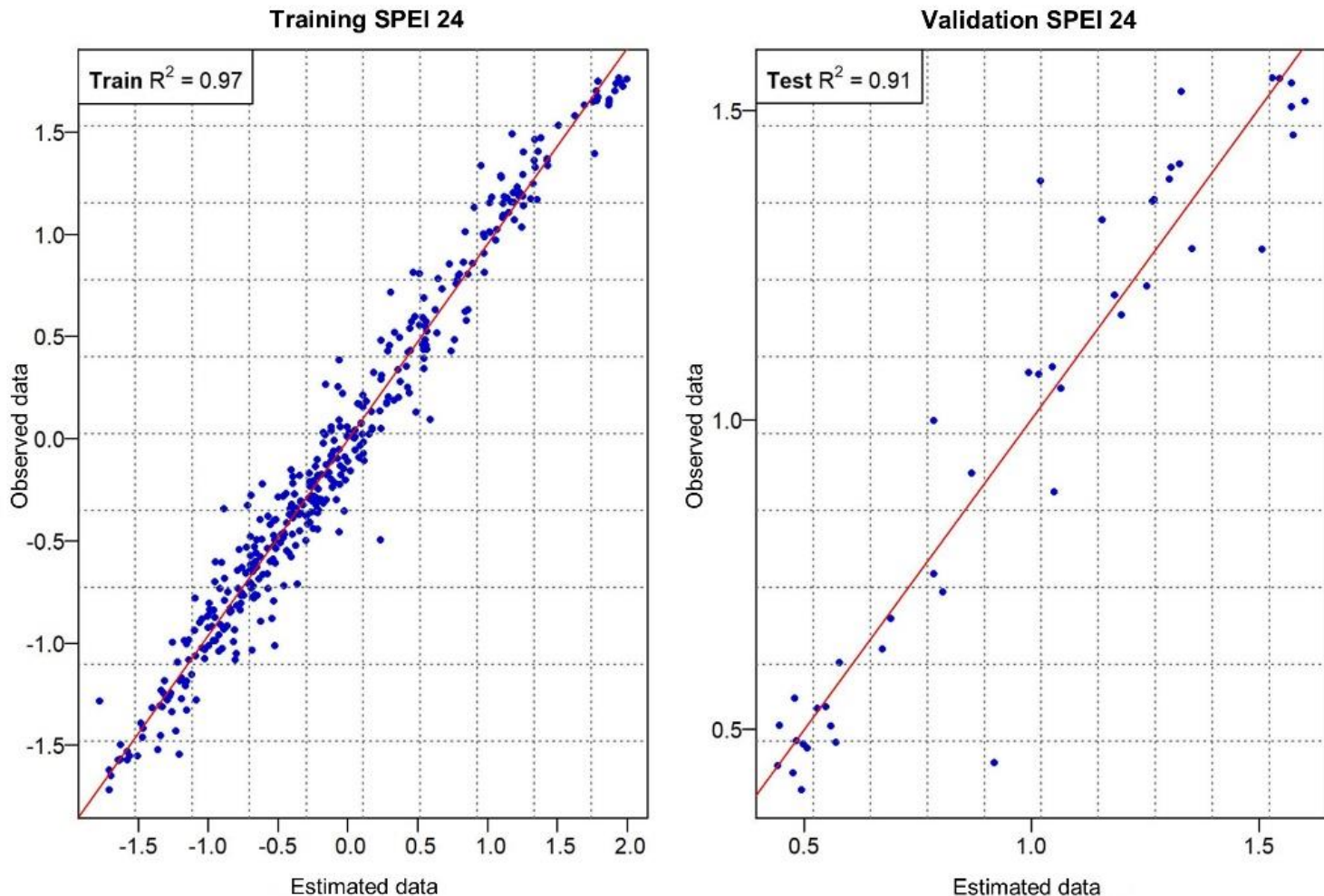


**Figure 7.** Training and validation of the neural network for SPEI 24 of group 2b.

According to the results of group 3 presented in Table 6, architectures 7-15-1 with *RPROP+* for SPI 24 and 5-10-1 with *RPROP-* for SPEI 24 were the best evaluated, with  $R^2 = 0.96$  in training. However, in the validation stage, architecture 12-16-1 with *RPROP+* for SPEI 12 was

that which obtained an  $R^2$  of 0.94 and had the best evaluation in this stage. When the values estimated by the neural network are compared with real data of the indexes in the complete data series, again, those that achieved the highest evaluations were the networks for SPI and SPEI at 24-month scales with  $E$  and  $R^2$  equal to 0.96. The results of this study agree with several studies, such as that conducted by Poornima and Pushpalatha (2019), who used recurrent neural networks and statistical models to predict drought using SPI and SPEI in the region of Hyderabad, India. They selected the neural network model with additional variables, such as temperature and relative humidity because it was superior in modeling droughts. The data used for calculating the indexes at different time scales (1, 5, and 12 months) were from 1975 to 2013. Azizi *et al.* (2019) evaluated the efficiency of artificial neural networks against a statistical method of mobile means to predict drought at the Ilam and Dehloran stations in Iran using SPI from the period 1983 to 2013).

**Table 6.** Optimal neural network models for group 3.

Index	Optimal architecture	Training Algorithm	Training			Validation			Complete Series		
			MSE	E	R <sup>2</sup>	MSE	E	R <sup>2</sup>	MSE	E	R <sup>2</sup>
SPI 3	7-8-1	RPROP+	0.009	0.62	0.62	0.005	0.70	0.71	0.272	0.63	0.63
SPI 6	12-17-1	RPROP-	0.006	0.87	0.87	0.003	0.83	0.83	0.100	0.87	0.87
SPI 12	12-15-1	RPROP-	0.004	0.91	0.91	0.002	0.87	0.88	0.070	0.90	0.90

SPI 24	7-15-1	<i>RPROP+</i>	0.002	0.96	0.96	0.001	0.90	0.90	0.033	0.96	0.96
SPEI 3	8-10-1	<i>RPROP+</i>	0.010	0.79	0.79	0.008	0.49	0.62	0.135	0.79	0.79
SPEI 6	12-19-1	<i>RPROP+</i>	0.004	0.90	0.90	0.003	0.90	0.90	0.060	0.90	0.90
SPEI 12	12-16-1	<i>RPROP+</i>	0.005	0.91	0.91	0.002	0.93	0.94	0.048	0.91	0.91
SPEI 24	5-10-1	<i>RPROP-</i>	0.002	0.96	0.96	0.001	0.77	0.80	0.020	0.96	0.96

They found that the ANN had higher predictive precision and that the most adequate architecture for predicting droughts at both stations was 5-30-1, according to their calculations of root mean square error, absolute mean error, and the coefficient of determination for the Ilam station, which was 0.60, 0.55 and 0.81 for training and 0.56, 0.46 and 0.93 validation, respectively. In contrast, the values at the Dehloran station were 0.60, 0.55, and 0.81 in training and 0.37, 0.28, and 0.99 in validation, respectively.

For group 3, Figure 8 presents the neural network that obtained the highest yield, with  $R^2 = 0.94$  during model validation, even though in training it had an  $R^2$  of 0.91 and was not the best evaluated in this stage (Figure 9). This network comprises 12 neurons in the input layer; that is, 12 delays in time were used to estimate the value of SPEI 12, and the hidden layer has a density of 16 neurons.

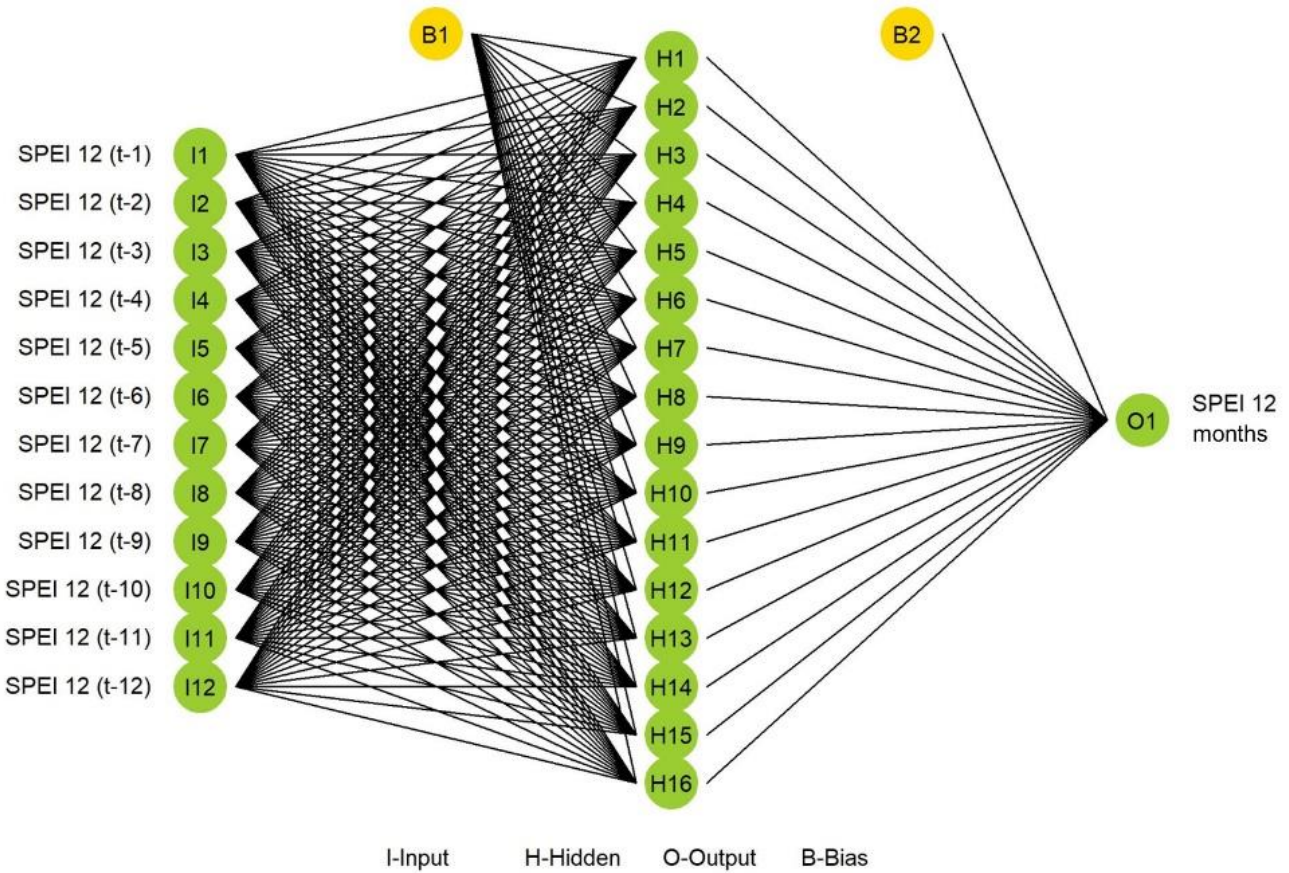


**Figure 8.** The architecture of the neural network for SPEI 12 of group 3.

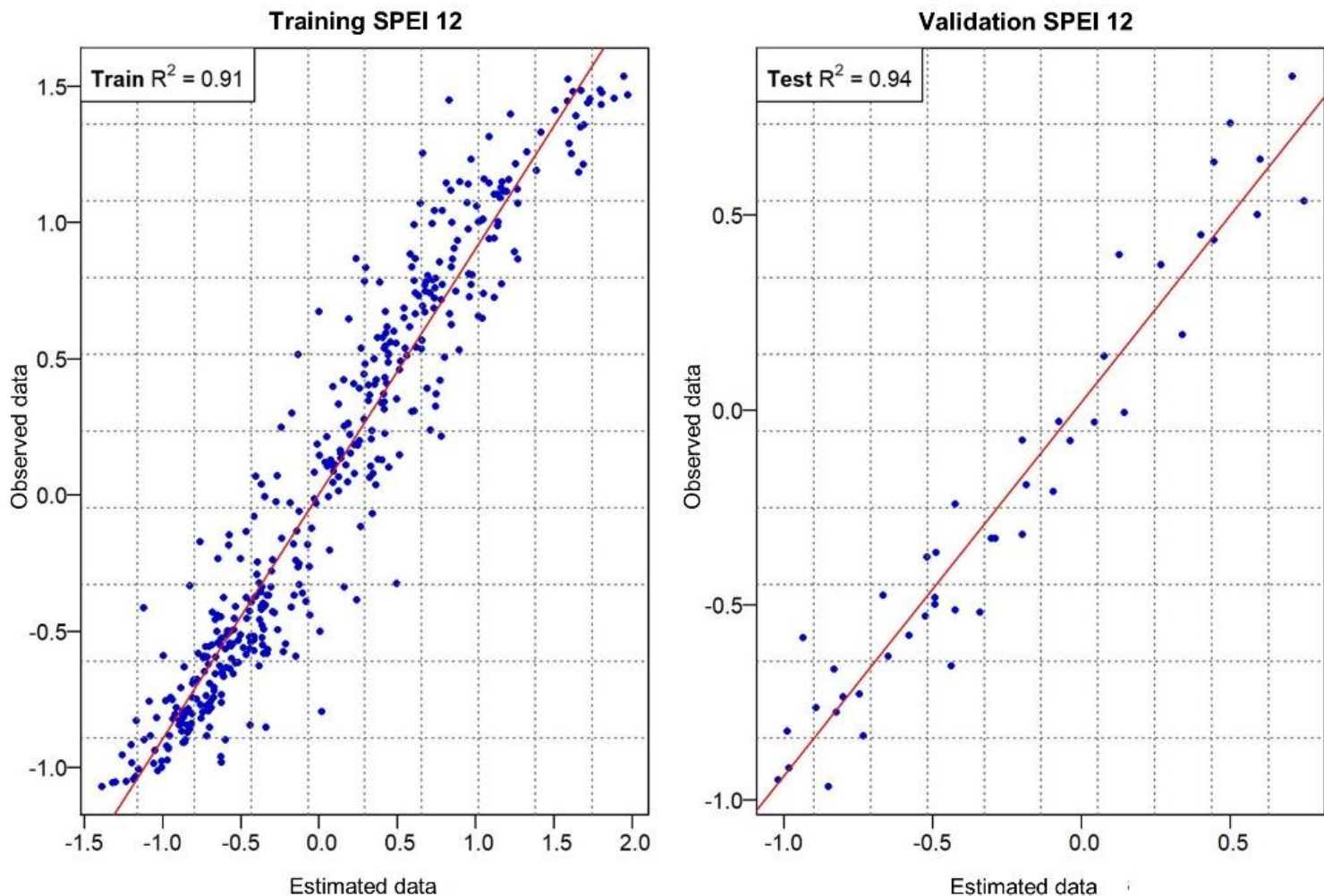


**Figure 9.** Training and validation of the neural network for SPEI 12 of group 3.

The analysis of SPI and SPEI carried out by Hernández-Vásquez *et al.* (2021) in the study area, group 2b showed the highest frequency of droughts occurred during the period from January 1974 to December

2013. They attributed this to the impact of diverse factors, such as relief and behavior of the wind systems. In this context, we can confirm that, of the study area, the region that covers the stations of group 2b is the most vulnerable to the impacts of droughts, and it is important to pay more attention to its behavior in the future. Figure 10 shows the behavior of the neural networks that obtained the best performance in each of the time scales used for this group during validation with the complete data series. According to the  $R^2$ , the forecast of SPEI was better than that of SPI and improved with longer time scales.

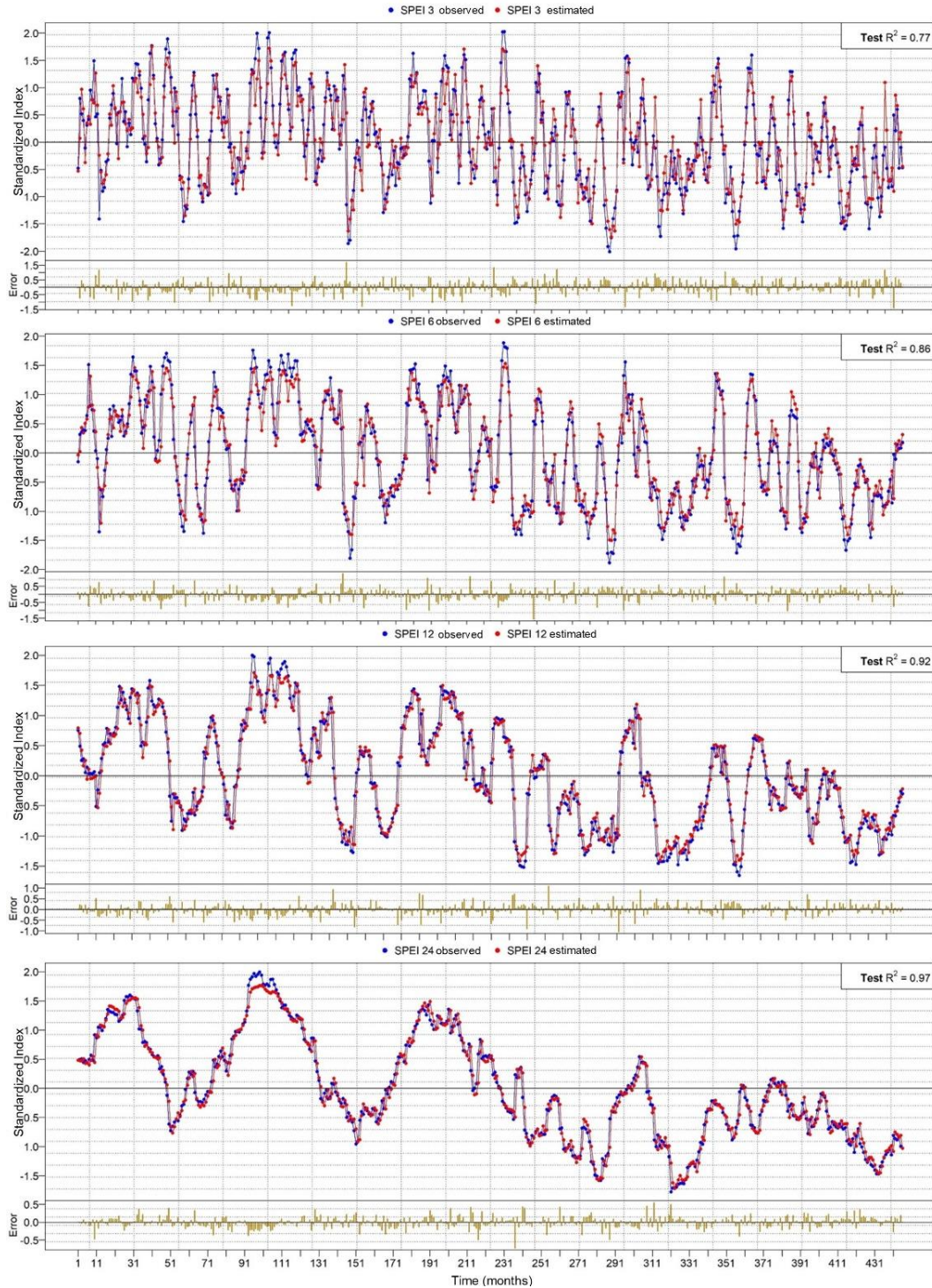


**Figure 10.** Observed and predicted SPEI for group 2b.

Table 7 presents the forecasts of the SPI and SPEI indexes for the three months following the study period: January, February, and March 2014. We compared them with the registers of the Mexico Drought Monitor (MSM) (Conagua & SMN, 2020), whose methodology is based on obtaining and interpreting seven different indexes and integrating them into a geographic information system, and the regions affected by drought are determined by consensus. According to the SPI and SPEI forecasts, the drought conditions in the study area oscillated between normal (N) and moderately dry (D1), except for the municipalities of Cananea and Bacoachi, located in the upper part of the basin, which had severe drought (D2) in the second half of March (Conagua & SMN, 2020). For group 1, the MSM declared that the conditions in January, February, and March were abnormally dry, coinciding with the forecasts of SPI 6 and SPEI 24 for group 2a and SPI 24 and SPEI 24 for group 2b. In the case of group 3, none of the forecasts coincided with those reported by MSM. However, with the SPI and SPEI indexes at 12- and 24-month scales, abnormally dry conditions were forecasted that approach those reported by Conagua and SMN (2020). In general, we observed in our study that using ANN for SPI forecasted less dry conditions than SPEI, which forecasted conditions that were closer to the real conditions, according to the MSM, and even closer when using 24-month scales.

**Table 7.** Forecasts of the SPI and SPEI indexes, from January to March 2014.

Group	Forecast 2014	MSM	SPI 3	SPEI 3	SPI 6	SPEI 6	SPI 12	SPEI 12	SPI 24	SPEI 24
1	January	D0	N	N	N	D0	N	D1	D0	D1
	February	D0	N	D0	N	D0	N	D0	D0	D1
	March	D0	N	D0	D0	D0	N	D0	D0	D1
2a	January	D1	N	D0	N	D0	N	D1	D0	D1
	February	D1	N	D1	D0	D1	D0	D1	D0	D1
	March	D1	N	D1	D1	D1	D0	D1	D0	D1
2b	January	D1	D0	N	N	N	N	N	D1	D1
	February	D1	D0	N	N	N	N	N	D1	D1
	March	D1	N	N	N	N	N	N	D1	D1
3	January	D1	N	N	N	N	D0	D0	D0	D0
	February	D1	N	N	D0	N	D0	D0	D0	D0
	March	D1	N	N	D0	D0	D0	D0	D0	D0
N= Normal conditions, D0= Abnormally dry, D1= Moderately dry										

## Conclusions

Using Cross-Validation, we determined the optimal architectures of the ANN models that achieved generalization of the observed data behavior without overfitting in the model behavior. The training was done with 90% of the data, and validation with the remaining 10%, and errors were relatively small. *MSE* did not surpass 0.015 in any of the evaluated cases.

In predicting drought indexes, we obtained  $R^2$  above 0.59 during training and 0.51 during validation. Thus, we can assert that the predictive ability of the ANN models was satisfactory.

ANN models were more precise in forecasting the indexes at scales of 24 months than at shorter time scales, possibly attributable to the high variability of hydro-climatic conditions in the short term. The predictive efficiencies of these models were superior in SPEI, demonstrating the importance of including evaporative demand in the moisture balance.

This study contributes a novel approach to drought forecasting, using analysis of SPI and SPEI and computer learning models with artificial neural networks. The results of this study are important and useful for planning and managing water resources in the study zone.

Future research on this topic should focus on analyzing the impact that forecasting and ANN model precision would have, including global-impact atmospheric phenomena, such as El Niño-Southern Oscillation, Pacific Decadal Oscillation, North Atlantic Oscillation, and climate change.

## Acknowledgements

Our thanks to Consejo Nacional de Ciencia y Tecnología (CONACyT) for the scholarship granted to carry out this study.

## References

- Achour, K., Meddi, M., Zeroual, A., Bouabdelli, S., Maccioni, P., & Moramarco, T. (2020). Spatio-temporal analysis and forecasting of drought in the plains of northwestern Algeria using the standardized precipitation index. *Journal of Earth System Science*, 129(1), 42. Recuperado de <https://doi.org/10.1007/s12040-019-1306-3>
- Anshuka, A., van Ogtrop, F. F., & Willem-Vervoort, R. (2019). Drought forecasting through statistical models using standardised precipitation index: A systematic review and meta-regression analysis. *Natural Hazards*, 97, 955-977. Recuperado de <https://doi.org/10.1007/s11069-019-03665-6>
- ASCE, American Society of Civil Engineers. (2000). Artificial neural networks in hydrology. I: Preliminary concepts. *Journal of Hydrologic Engineering*, 5(2), 115-123.
- Azizi, E., Tavakoli, M., Karimi, H., & Faramarzi, M. (2019). Evaluating the efficiency of the neural network to other methods in predicting drought in arid and semi-arid regions of western Iran. *Arabian Journal*

of *Geosciences*, 12(15). Recuperado de  
<https://doi.org/10.1007/s12517-019-4654-z>

Bari-Abarghouei, H., Reza-Kousari, M., & Asadi-Zarch, M. A. (2013). Prediction of drought in dry lands through feedforward artificial neural network abilities. *Arabian Journal of Geosciences*, 6(5), 1417-1433. Recuperado de <https://doi.org/10.1007/s12517-011-0445-x>

Beguería, S., & Vicente-Serrano, S. M. (2017). *Calculation of Standardised Precipitation-Evapotranspiration Index*, (1.7)(Issue June). Recuperado de <http://sac.csic.es/spei>

Campos-Aranda, D. F. (1998). *Procesos del ciclo hidrológico* (3a ed.). San Luis Potosí, México: Facultad de Ingeniería, Universidad Autónoma de San Luis Potosí.

Castillo-Castillo, M., Ibáñez-Castillo, L. A., Valdés, J. B., Arteaga-Ramírez, R., & Vázquez-Peña, M. A. (2018). Pronóstico de sequías meteorológicas con filtro de Kalman discreto en la cuenca del río Fuerte, México. *Agrociencia*, 52(7), 911-932.

Cervantes-Osornio, R., Arteaga-Ramírez, R., Vázquez-Peña, M. A., Ojeda-Bustamante, W., & Quevedo-Nolasco, A. (2013). Modelos Hargreaves Priestley-Taylor y redes neuronales artificiales en la estimación de la evapotranspiración de referencia. *Ingeniería, Investigación y Tecnología*, 14(2), 163-176. Recuperado de  
[https://doi.org/10.1016/s1405-7743\(13\)72234-0](https://doi.org/10.1016/s1405-7743(13)72234-0)

Choubin, B., Malekian, A., & Golshan, M. (2016). Application of several data-driven techniques to predict a standardized precipitation index. *Atmosfera*, 29(2), 121-128. Recuperado de <https://doi.org/10.20937/ATM.2016.29.02.02>

Conagua & SMN, Comisión Nacional del Agua & Servicio Meteorológico Nacional. (2020). *Monitor de Sequía de México (MSM)*. Recuperado de <https://smn.conagua.gob.mx/es/climatologia/monitor-de-sequia/monitor-de-sequia-en-mexico>

Djerbouai, S., & Souag-Gamane, D. (2016). Drought forecasting using neural networks, wavelet neural networks, and stochastic models: Case of the algerois basin in North Algeria. *Water Resources Management*, 30(7), 2445-2464. Recuperado de <https://doi.org/10.1007/s11269-016-1298-6>

El-Ibrahimi, A., & Baali, A. (2018). Application of several artificial intelligence models for forecasting meteorological drought using the standardized precipitation index in the Saïss Plain (Northern Morocco). *International Journal of Intelligent Engineering and Systems*, 11(1), 267-275. Recuperado de <https://doi.org/10.22266/ijies2018.0228.28>

Gallegos-Cedillo, J., Arteaga-Ramírez, R., Vázquez-Peña, M. A., & Juárez-Méndez, J. (2016). Estimation of missing daily precipitation and maximum and minimum temperature records in San Luis Potosí. *Ingeniería Agrícola y Biosistemas*, 8(1), 3-16. Recuperado de <https://doi.org/10.5154/r.inagbi.2015.11.008>

Gómez-Guerrero, J. S., & Aguayo-Arias, M. I. (2019). Performance evaluation of rainfall data fill-in methods in two morphostructural areas of south-central Chile. *Investigaciones Geográficas*, 99. Recuperado de <https://doi.org/10.14350/rig.59837>

Günther, F., & Fritsch, S. (2010). Neuralnet: Training of neural networks. *R Journal*, 2(1), 30-38. Recuperado de <https://doi.org/10.32614/rj-2010-006>

Haykin, S. (1998). *Neural networks: A comprehensive foundation* (2<sup>nd</sup> ed.). Ontario, Canadá: Prentice Hall.

Hernández-Vásquez, C. C., Ibáñez-Castillo, L. A., Gómez-Díaz, J. D., & Arteaga-Ramírez, R. (2021). Analysis of meteorological droughts in the Sonora River Basin, Mexico. *Atmósfera*. Recuperado de <https://doi.org/https://doi.org/10.20937/ATM.52954>

Khan, M. M. H., Muhammad, N. S., & El-Shafie, A. (2018). Wavelet-ANN versus ANN-based model for hydrometeorological drought forecasting. *Water (Switzerland)*, 10(8), 1-21. Recuperado de <https://doi.org/10.3390/w10080998>

Laqui, W., Zubietta, R., Rau, P., Mejía, A., Lavado, W., & Ingol, E. (2019). Can artificial neural networks estimate potential evapotranspiration in Peruvian highlands? *Modeling Earth Systems and Environment*, 5(4), 1911-1924. Recuperado de <https://doi.org/10.1007/s40808-019-00647-2>

Martín-del-Brio, B., & Sanz-Molina, A. (2001). *Redes neuronales y sistemas difusos*. Bogotá, Colombia: Alfaomega.

McCulloch, W. S., & Pitts, W. (1943). A logic calculus of the ideas immanent in nervous activity. *Bulletin of Mathematical Biophysics*, 5, 115-133. Recuperado de <https://doi.org/10.1007/BF02478259>

McKee, T. B., Doesken, N. J., & John, K. (1993). The relationship of drought frequency and duration to time scales. *Eighth Conference on Applied Climatology*, 17-22.

Mishra, A. K., & Desai, V. R. (2006). Drought forecasting using feed-forward recursive neural network. *Ecological Modelling*, 198(1-2), 127-138. Recuperado de <https://doi.org/10.1016/j.ecolmodel.2006.04.017>

Mishra, A. K., & Singh, V. P. (2011). Drought modeling - A review. *Journal of Hydrology*, 403(1-2), 157-175. Recuperado de <https://doi.org/10.1016/j.jhydrol.2011.03.049>

Mouatadid, S., Raj, N., Deo, R. C., & Adamowski, J. F. (2018). Input selection and data-driven model performance optimization to predict the Standardized Precipitation and Evaporation Index in a drought-prone region. *Atmospheric Research*, 212(May), 130-149. Recuperado de <https://doi.org/10.1016/j.atmosres.2018.05.012>

Oertel, M., Meza, F. J., Gironás, J., Scott, C. A., Rojas, F., & Pineda-Pablos, N. (2018). Drought propagation in semi-arid river basins in Latin America: Lessons from Mexico to the Southern Cone. *Water*

(Switzerland), 10(11), 1-21. Recuperado de  
<https://doi.org/10.3390/w10111564>

OMM, Organización Meteorológica Mundial. (2011). Guía de prácticas climatológicas. Vol. 100. Ginebra, Suiza: Organización Meteorológica Mundial.

OMM & GWP, Organización Meteorológica Mundial & Asociación Mundial para el Agua. (2016). Manual de indicadores e índices de sequía. En: *Programa de gestión integrada de sequías. Serie 2 de herramientas y directrices para la gestión integrada de sequías*. Ginebra/Estocolmo, Suiza: Organización Meteorológica Mundial y Asociación Mundial para el Agua.

Ortíz, D., Villa, F., & Velásquez, J. (2007). A comparison between evolutionary strategies and RPROP for estimating neural networks. *Avances e Sistemas e Informática*, 4(2), 135-144.

Palma, A., González, F., & Cruickshank, C. (2015). Managed aquifer recharge as a key element in Sonora River basin management, Mexico. *Journal of Hydrologic Engineering*, 20(3), 1-10. Recuperado de [https://doi.org/10.1061/\(ASCE\)HE.1943-5584.0001114](https://doi.org/10.1061/(ASCE)HE.1943-5584.0001114)

Poornima, S., & Pushpalatha, M. (2019). Drought prediction based on SPI and SPEI with varying timescales using LSTM recurrent neural network. *Soft Computing*, 23(18), 8399-8412. Recuperado de <https://doi.org/10.1007/s00500-019-04120-1>

Prasad, N., Singh, R., & Lal, S. P. (2013). Comparison of back propagation and resilient propagation algorithm for spam classification.

*Proceedings of International Conference on Computational Intelligence, Modelling and Simulation* (pp. 29-34). Recuperado de <https://doi.org/10.1109/CIMSim.2013.14>

Ravelo, A. C., Sanz-Ramos, R., & Douriet-Cárdenas, J. C. (2014). Detección, evaluación y pronóstico de las sequías en la región del Organismo de Cuenca Pacífico Norte, México. *Agriscientia*, 31(1), 11-24.

Rezaeian-Zadeh, M., & Tabari, H. (2012). MLP-based drought forecasting in different climatic regions. *Theoretical and Applied Climatology*, 109(3-4), 407-414. Recuperado de <https://doi.org/10.1007/s00704-012-0592-3>

Riedmiller, M. (1994). Advanced supervised learning in multi-layer perceptron's - from backpropagation to adaptive learning algorithms. *International Journal of Computer Standards and Interfaces*, 16, 265-278.

Riedmiller, M., & Braun, H. (1993). A direct adaptive method for faster backpropagation learning: The RPROP algorithm. *Proceedings of the IEEE International Conference on Neural Networks (ICNN)* (pp. 586-591). Recuperado de <https://doi.org/10.1109/icnn.1993.298623>

RStudio. (2018). *RStudio: Integrated Development Environment for R*. RStudio, Inc. Recuperado de <http://www.rstudio.com/>

SMN, Servicio Meteorológico Nacional. (2019). *Red de Estaciones Climatológicas. Climatología mensual*. Ciudad de México, México: Servicio Meteorológico Nacional. Recuperado de <http://smn1.conagua.gob.mx/climatologia/Mensuales/>

Soh, Y. W., Koo, C. H., Huang, Y. F., & Fung, K. F. (2018). Application of artificial intelligence models for the prediction of standardized precipitation evapotranspiration index (SPEI) at Langat River Basin, Malaysia. *Computers and Electronics in Agriculture*, 144(May 2017), 164-173. Recuperado de <https://doi.org/10.1016/j.compag.2017.12.002>

Vargas-Castañeda, G., Ibáñez-Castillo, L. A., & Arteaga-Ramírez, R. (2015). Development, classification, and trends in rainfall-runoff modeling. *Ingeniería Agrícola y Biosistemas*, 7(1), 5-21. Recuperado de <https://doi.org/10.5154/r.inagbi.2015.03.002>

Velásquez, J. D., Fonseca, Y., & Villa, F. A. (2013). Pronóstico de series de tiempo con redes neuronales regularizadas y validación cruzada. *Revista Vínculos*, 10(1), 267-279.

Velásquez, J. D., Villa, F. A., & Souza, R. C. (2010). Time series forecasting using cascade correlation networks. *Ingeniería e Investigación*, 30(1), 157-162.

Vicente-Serrano, S. M., Beguería, S., & López-Moreno, J. I. (2010). A multiscalar drought index sensitive to global warming: The standardized precipitation evapotranspiration index. *Journal of*

*Climate*, 23(7), 1696-1718. Recuperado de  
<https://doi.org/10.1175/2009JCLI2909.1>

Villazón-Bustillos, D., Rubio-Arias, H. O., Ortega-Gutiérrez, J. A., Rentería-Villalobos, M., González-Gurrula, L. C., & Pinales-Munguia, A. (2016). Análisis en series de tiempo para el pronóstico de sequía en la región noroeste del estado de Chihuahua. *Ecosistemas y Recursos Agropecuarios*, 3(9), 307-315.

Wilhite, D. A., & Glantz, M. H. (1985). Understanding the drought phenomenon: The role of definitions. *Water International*, 10(3), 111-120. Recuperado de <https://doi.org/10.1080/02508068508686328>

Zhang, R., Chen, Z. Y., Xu, L. J., & Ou, C. Q. (2019). Meteorological drought forecasting based on a statistical model with machine learning techniques in Shaanxi province, China. *Science of the Total Environment*, 665, 338-346. Recuperado de  
<https://doi.org/10.1016/j.scitotenv.2019.01.431>